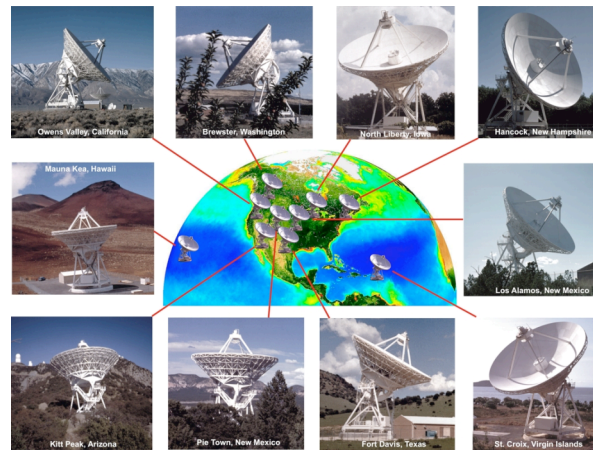
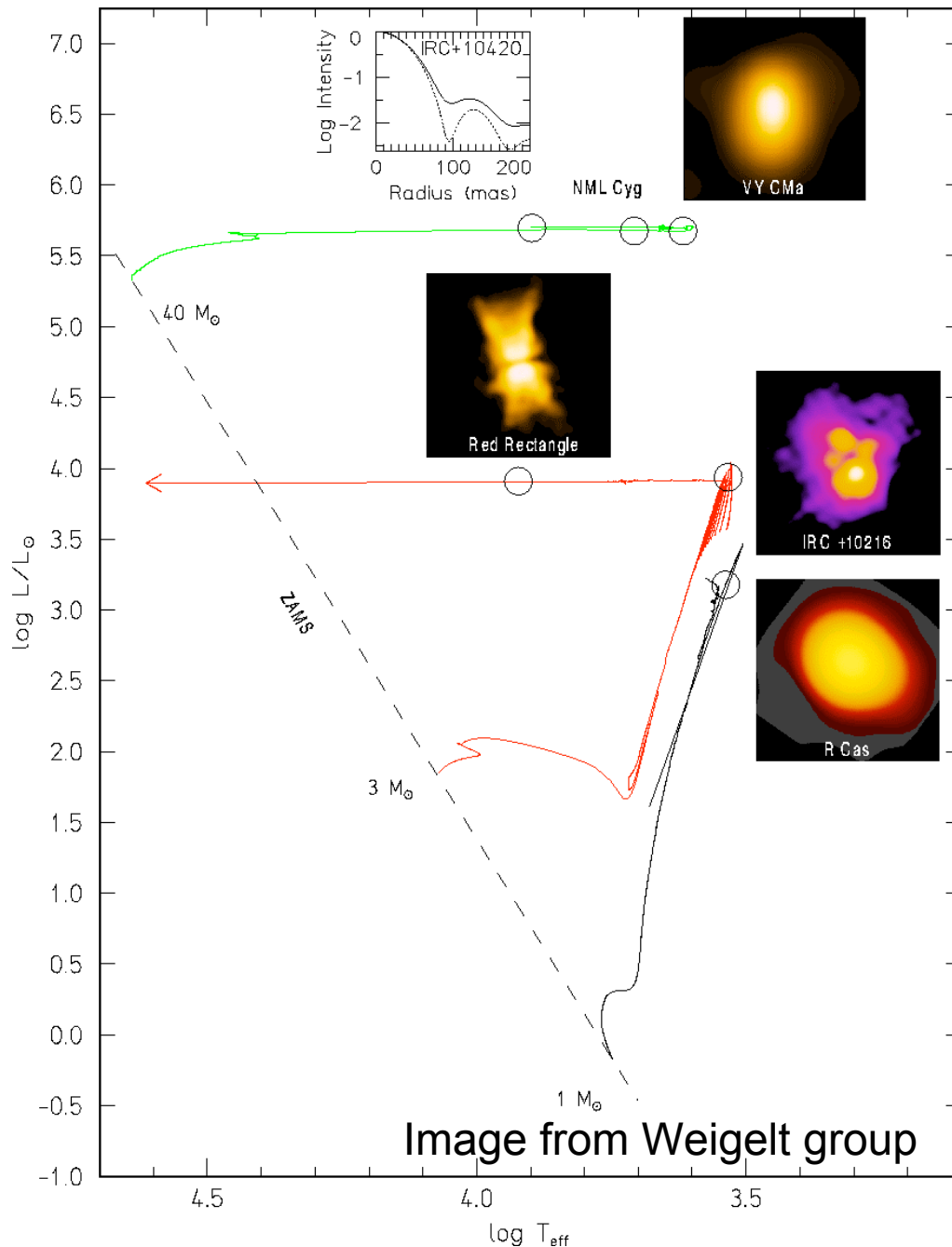


# Atmospheres, pulsation, and mass-loss of AGB stars and supergiants



Markus Wittkowski (ESO)

In collaboration with David A. Boboltz (USNO), Keiichi Ohnaka, Thomas Driebe (MPIfR Bonn), Michael Scholz (Univ. Heidelberg/ Univ. Sydney)



Atmospheres, pulsation, and mass-loss of AGB stars

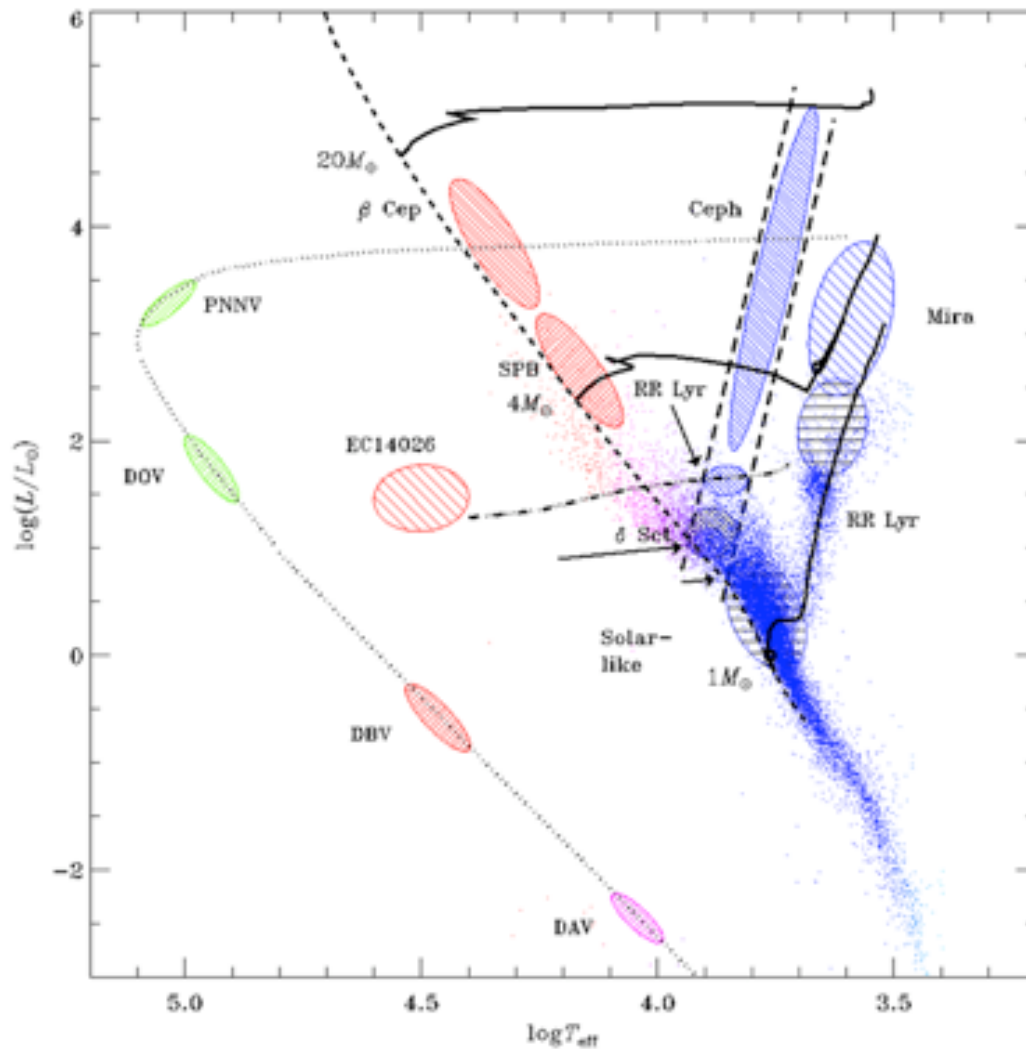
AGB phase is accompanied by significant mass loss to the circumstellar environment.

Mass-loss affects any further stellar evolution and is one of the most important sources for the chemical enrichment of the interstellar medium.

Its details are not well understood, in particular the driving mechanism for the acceleration of the innermost dust for oxygen-rich stars, and the connection between stellar pulsation and mass-loss.

Another unknown is how spherically symmetric stars evolve to form axisymmetric Pne.

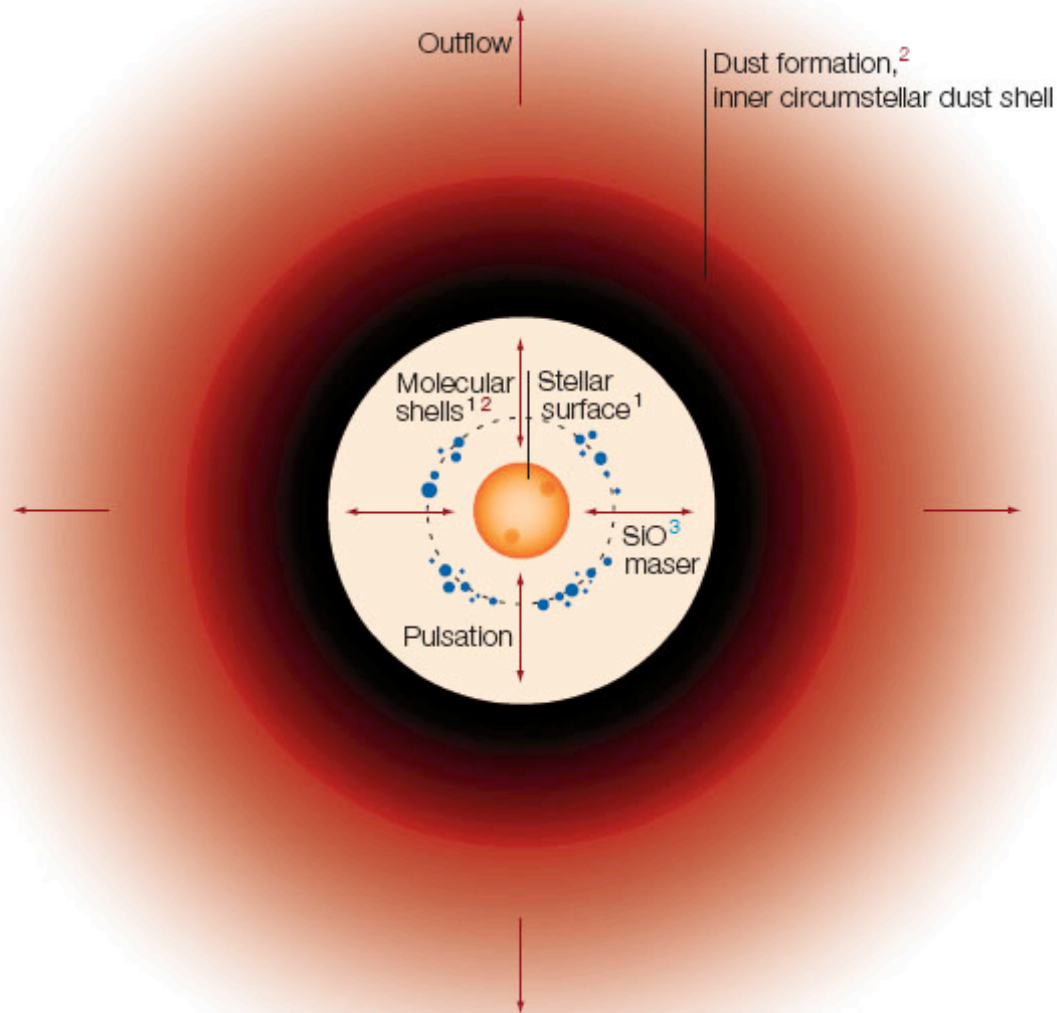
# Stellar pulsation in the HR diagram



Regions of mass-loss in the HR diagram may fall together with regions of stellar pulsation.

Fig. from J. Christensen-Dalsgaard.

# Sketch of an oxygen-rich Mira star



## Polychromatic interferometry:

- NIR: photosphere
- MIR: molecular shell
- 7mm: SiO maser shell
- MIR: inner dust shell
- 1.3cm: Wind region (H<sub>2</sub>O maser)

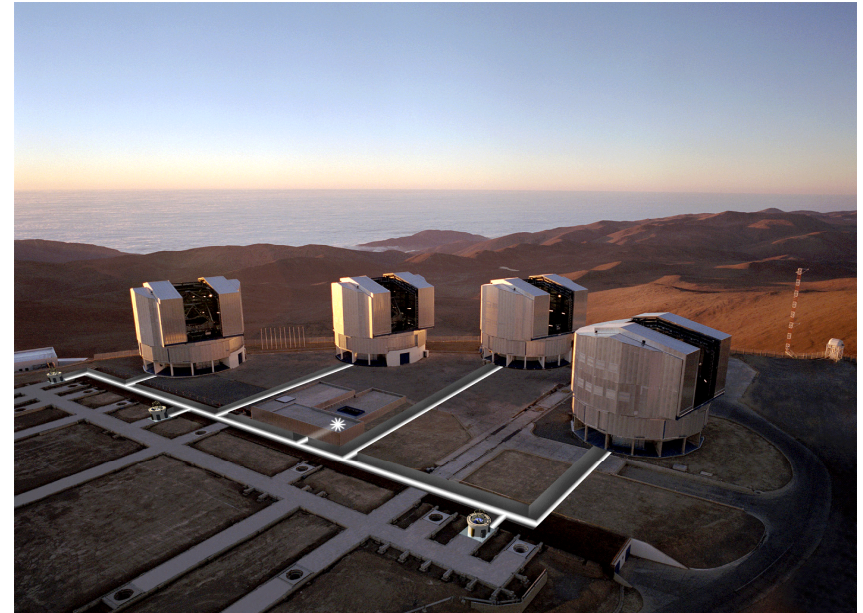
H<sub>2</sub>O maser<sup>3</sup>  
(20-50 R<sub>\*</sub>)

OH maser<sup>3</sup>  
(200-500 R<sub>\*</sub>)

<sup>1</sup>AMBER  
<sup>2</sup>MIDI  
<sup>3</sup>VLBA/MERLIN

# The ESO VLT Interferometer

- Four fixed 8-m Unit Telescopes (UTs). Max. Baseline 130m.
  - Four 1.8-m Auxiliary Telescopes (ATs), relocateable on 30 different stations. Baselines 8 – 200m.
  - Near-infrared (J, H, K) closure-phase instrument AMBER. Spectral resolutions 35, 1500, 10000.
  - Mid-infrared 8-13  $\mu\text{m}$  2-beam instrument MIDI. Spectral resolutions 30, 230.
  - Fringe tracker (FINITO).
  - Dual feed phase referencing (PRIMA).
- 
- Dual feed phase referencing (PRIMA).



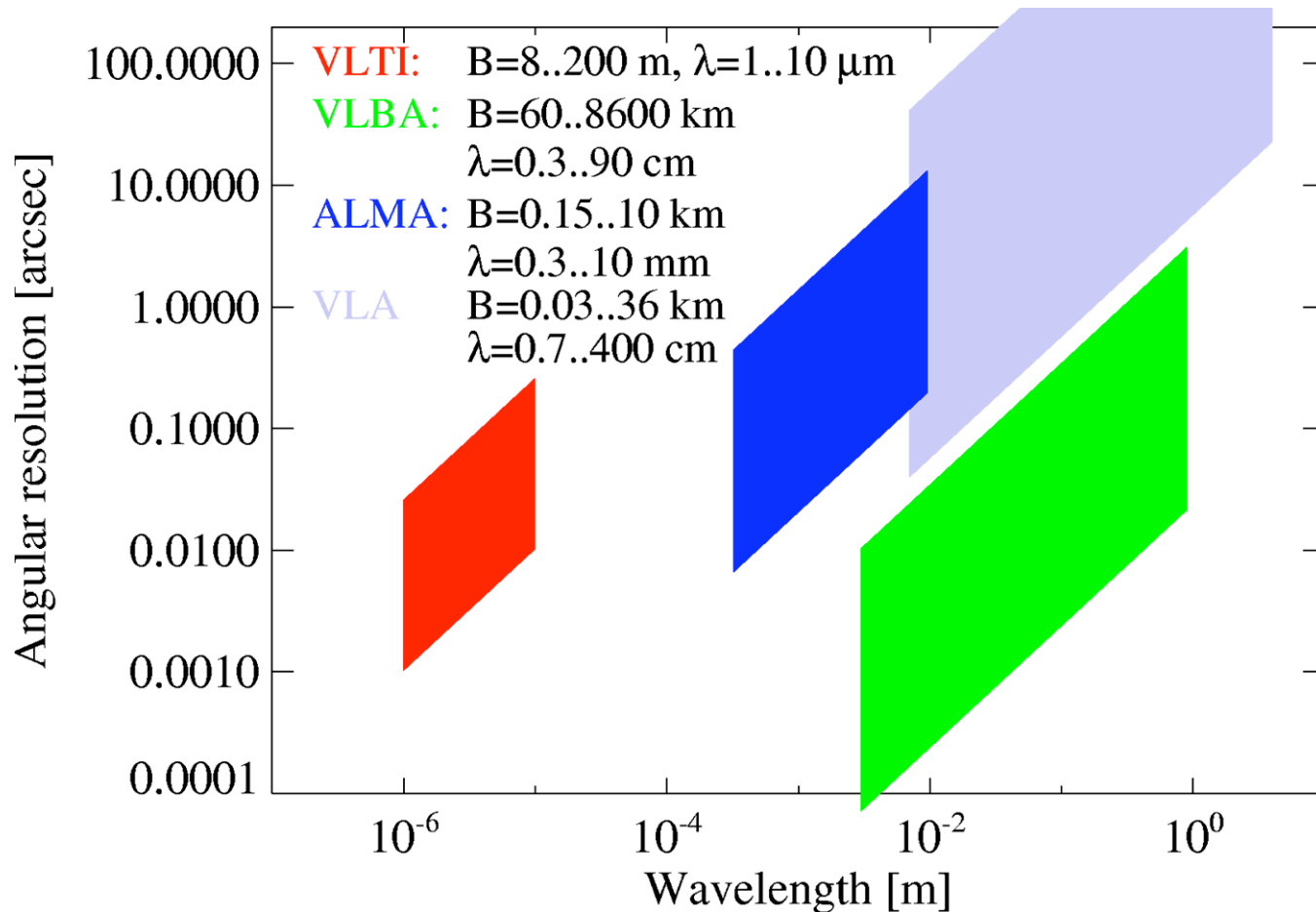
AT1 and AT2 with Open Domes

# Maser observations with the VLBA

- AGB stars exhibit SiO, OH, and H<sub>2</sub>O maser emission, probing the stellar environment from inside the dust formation point all the way to the outer regions of the wind.
- The VLBA is a system of ten 25m radio telescopes; 0.3-90 GHz, angular resolution down to sub-milli-arcsecond.
- The maser emission can well be spatially resolved with the VLBA.
- Maser radiation appears in maser spots, each with its own well-defined velocity, related to molecular clouds of common velocity with certain temperature and density conditions.
- Each spot emits beamed radiation to the observer.
- SiO masers are tangentially amplified with respect to the stellar radiation, leading to ring-like structures.



# Comparison of VLTI, VLBA, and ALMA



- VLTI, VLBA, and ALMA can observe the same targets in terms of angular resolution and sensitivity.
- They provide complementary information on different components and regions.

## Telescopes:

**VLTI** : 4 x 8m + 4 x 1.8 m

**VLBA** : 10 x 25 m

**ALMA** : 64 x 12 m

**VLA** : 27 x 25 m

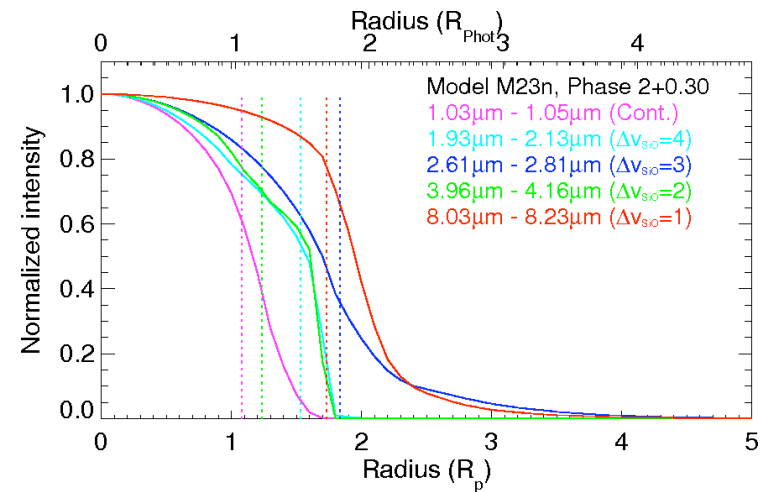
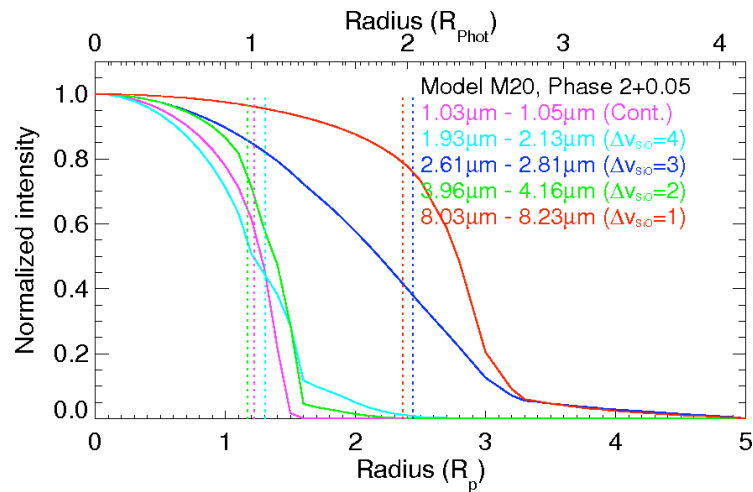
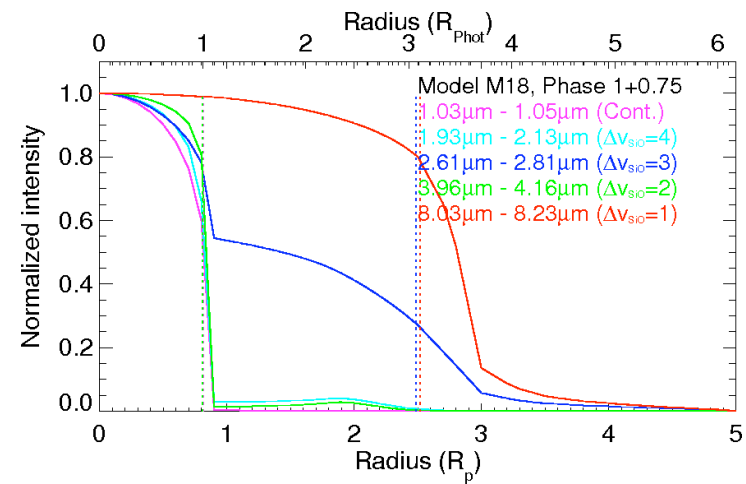
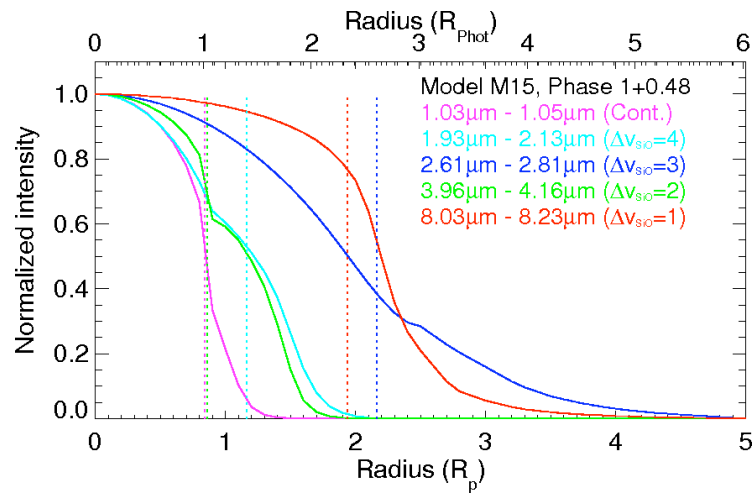
# Project description

- **Goal:** Better understanding of the mass-loss process from evolved stars and its connection to stellar pulsation.
- **Method:** Use two of the highest resolution interferometers in the world, the Very Large Telescope Interferometer (VLTi) and the Very Long Baseline Array (VLBA) to study Asymptotic Giant Branch (AGB) stars and supergiants and their circumstellar envelopes.
- **Source Selection:** We have thus far concentrated on 4 stars, S Ori, GX Mon, RR Aql, and AH Sco. These stars were selected to be observable with the VLBA in the northern hemisphere and the VLTi in the southern hemisphere. All stars except S Ori have both SiO and H<sub>2</sub>O maser emission (S Ori has only SiO).

# Modeling of the infrared interferometric data

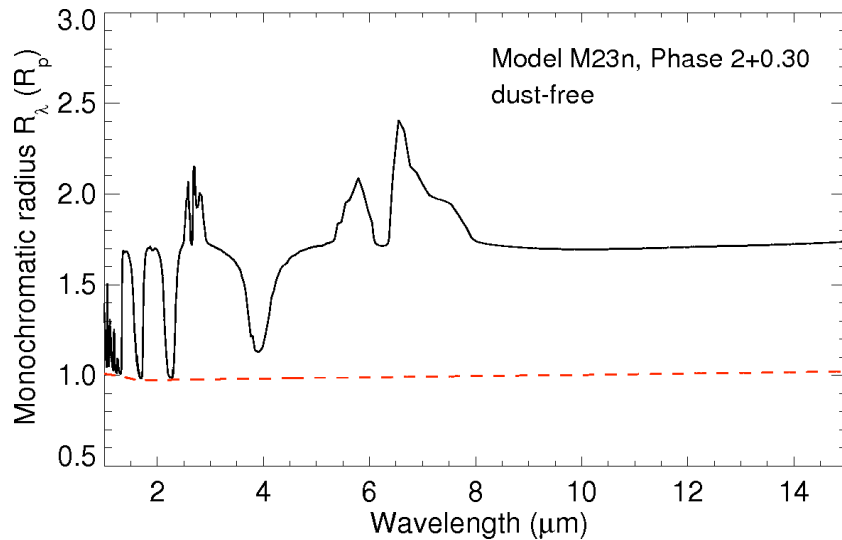
- We model the **stellar atmosphere** using Scholz & Wood models: **P and M series** (Ireland et al. 2004a/b). These are complete self-excited dynamic model atmospheres of Mira stars that include the effects from molecular layers lying above the continuum-forming layers.
- We model the **dust shell** using the **radiative transfer code mcsim\_mpi** (Ohnaka et al. 2006). Dust chemistry follows the work by Lorenz-Martins & Pompeia (2000): IRAS LRS spectra of AGB stars can be described by shells of  $\text{Al}_2\text{O}_3$  grains, silicate grains, or a mix thereof.  
S Ori:  $\text{Al}_2\text{O}_3$  grains alone, confirmed by our study.
- Model parameters: Model phase;  $R_{\text{in}}$ ,  $\tau_{\text{V}}$ , density gradient  $\rho$ ;  $\Theta_{\text{phot}}$  fitted.

# CLVs as function of phase and bandpass

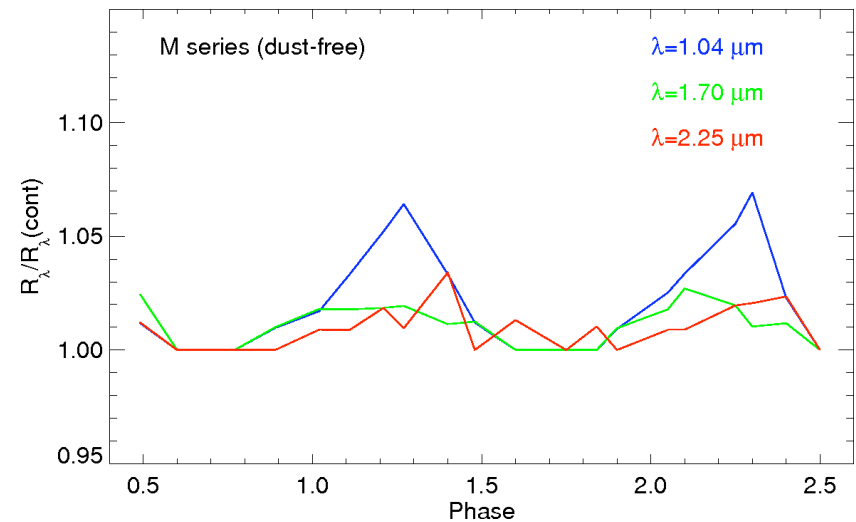


# The photospheric continuum radius

Radius  $R_\lambda(\tau_\lambda=1)$  for one phase as function of wavelength:



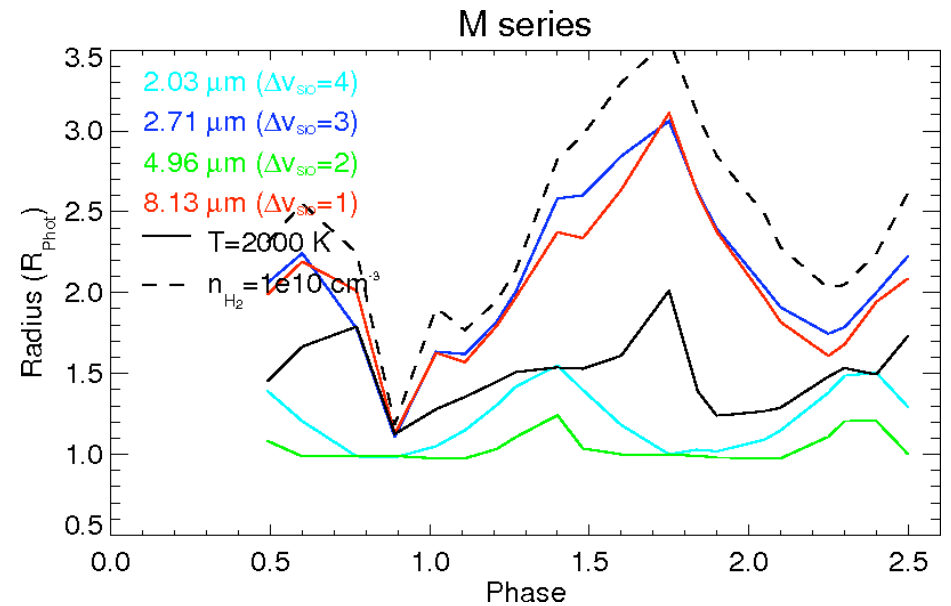
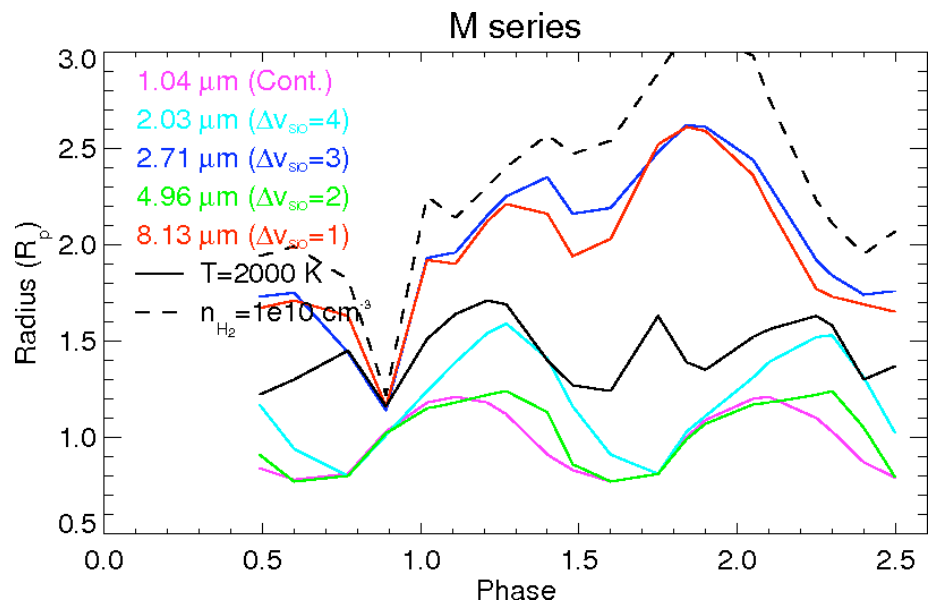
Radius at different continuum bands as a function of cycle/phase:



$R_\lambda$  shows strong variations in the range  $1-8 \mu\text{m}$ , and an approx. constant shape between  $8$  and  $15 \mu\text{m}$  at roughly  $2 R_{\text{cont}}$  caused by water layers.

Continuum contamination depends strongly on both wavelength and phase, and different near-continuum bandpass radii may be closest to the pure-continuum radius at different phases.

# Radii at different bandpasses



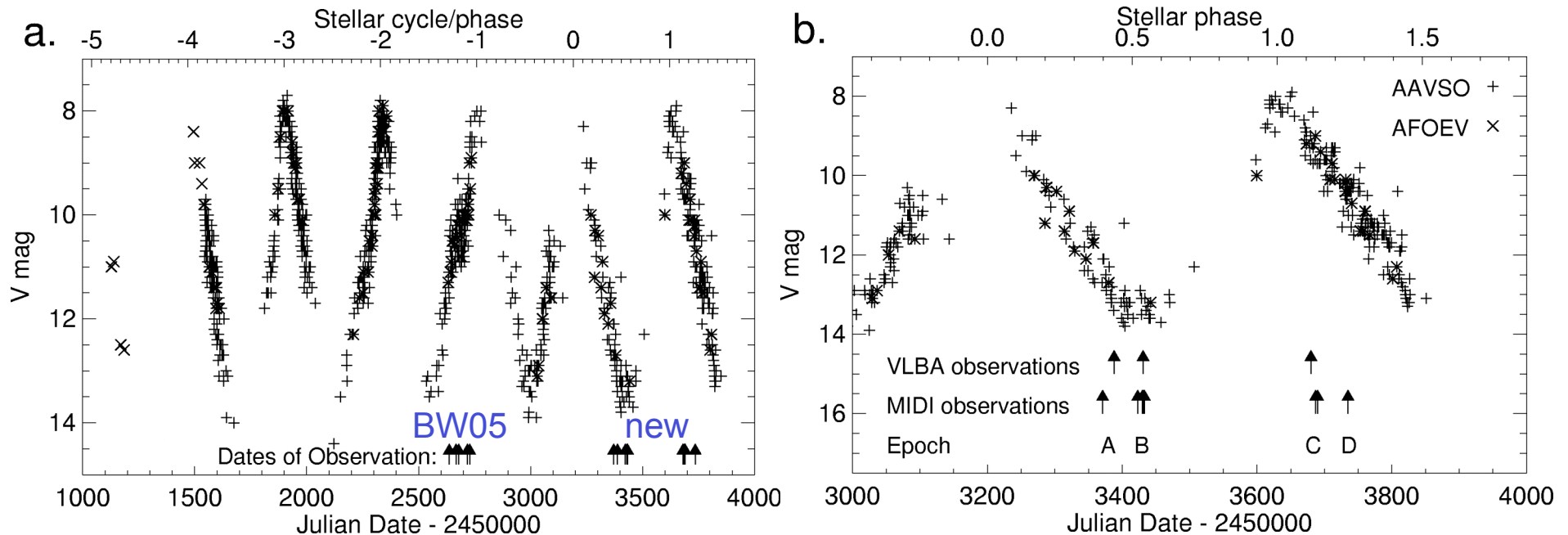
Radii of constant temperature or density or at certain bandpasses show variation but not a clear correlation with phase for the M model series.

# Basic uncertainties in VLTI/VLBA studies of the atmosphere and the CSE of evolved stars

- In practice, observational bandpasses in the infrared include a blend of photons arriving from the photosphere and from overlying molecular shells.
  - > Use of atmosphere models to relate the observed data to a well defined Rosseland-mean or continuum diameter.
  - > Observe in narrow continuum bands or with high spectral resolution.
- For pulsating stars, the relative positions between different layers are expected to change with stellar phase and cycle.
  - > Time series of concurrent observations.
- Astrometric information between observations at different facilities and wavelengths is often lost (e.g. between VLBA and VLTI observations).
  - > Astrometry with respect to the same reference source (not yet possible with VLTI, but will be with the PRIMA facility).
- Asymmetric structures might be expected already on the AGB, but models are spherical, and asymmetric structures are difficult to probe with a 2-beam instrument like MIDI.

# Concurrent VLT/ VLBA observations of S Ori

S Ori : M6.5e-M9.5e; V=7.2-14.0; P~430d; d~480 pc; SiO and OH maser



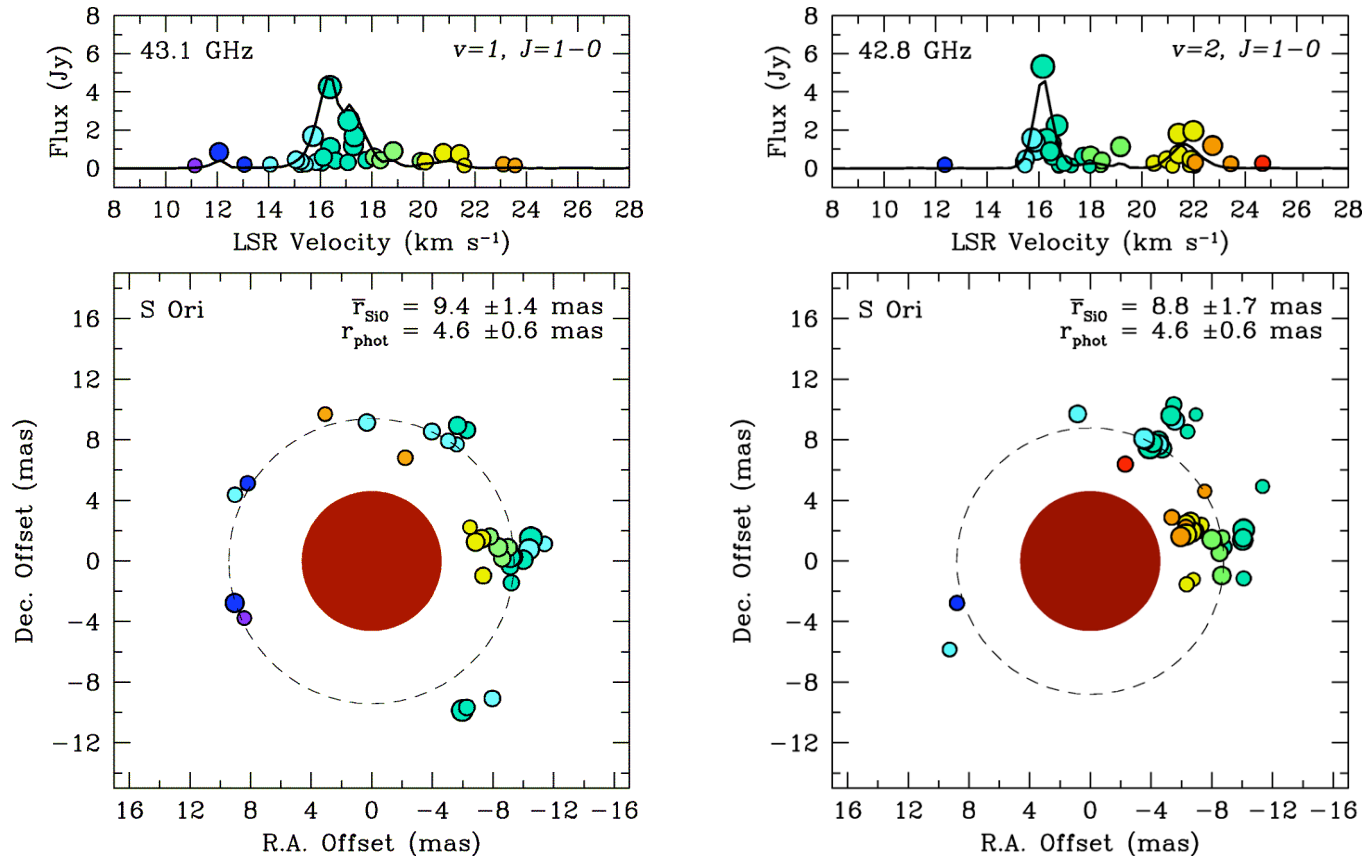
First coordinated VLT/ VLBA observations:  
 VINCI: 25 Jan – 31 Mar 2003, phases 0.80 - 0.95.  
 VLBA : 29 Dec 2002, phase 0.73

Boboltz & Wittkowski 2005

New VLT/ MIDI and VLBA observations:  
 3 contemporaneous (differences < 0.04  $P$ ) epochs  
 between Dec 2004 and Nov. 2005 at phases 0.44, 0.56, 1.15, (1.27).

Wittkowski et al. 2007

# VINCI and VLBA observations of S Ori (BW05)



VLTI/VINCI data: K-band UD diameter 10.5 mas (phase 0.80) - 10.2 mas (0.95).

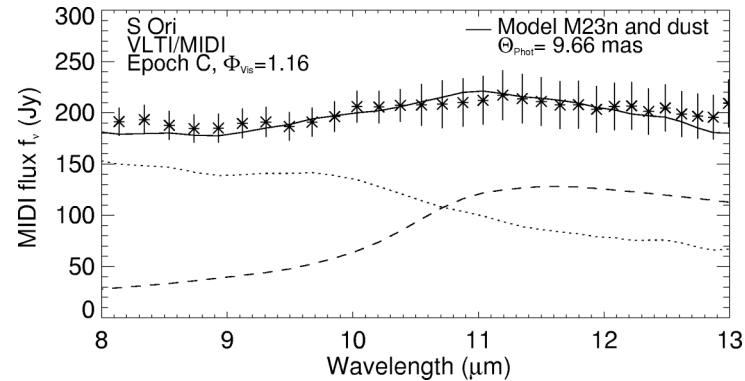
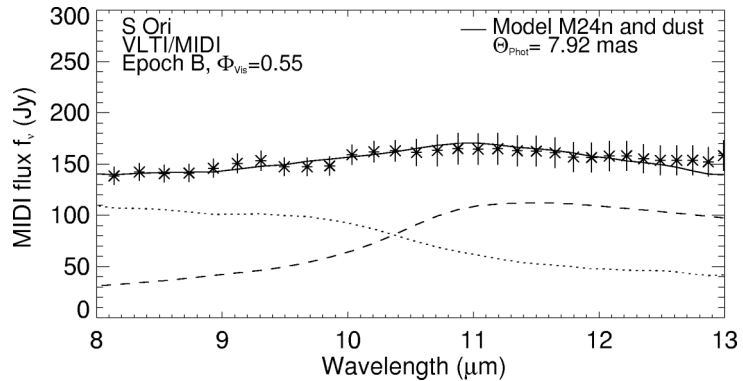
Extrapolation to phase 0.73 and correction  $\Theta_{\text{UD/cont}} \Rightarrow \Theta_{\text{cont}} = 9.2 \text{ mas}$

SiO maser ring radius:  $2.0 R_*$  (43.1 GHz) and  $1.9 R_*$  (42.8 GHz) at stellar phase 0.73, free of the usual uncertainty inherent in comparing observations widely spaced in phase.

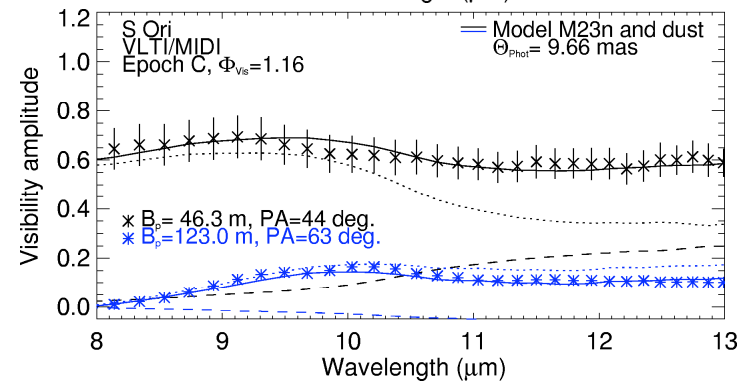
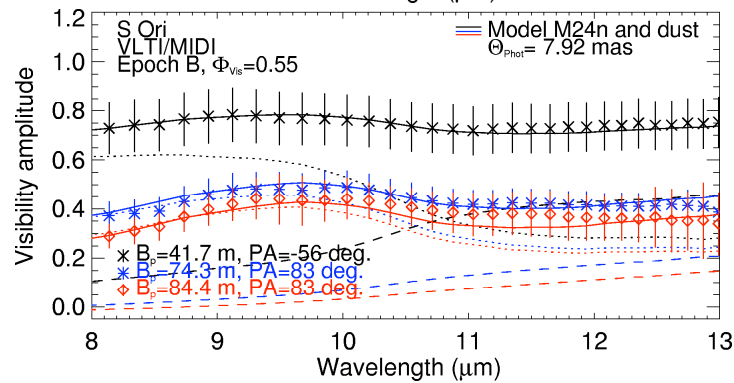
Boboltz & Wittkowski 2005

19 November 2007, Nice, France

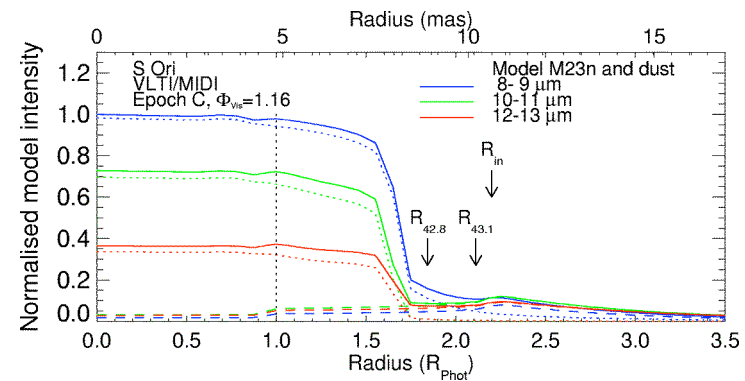
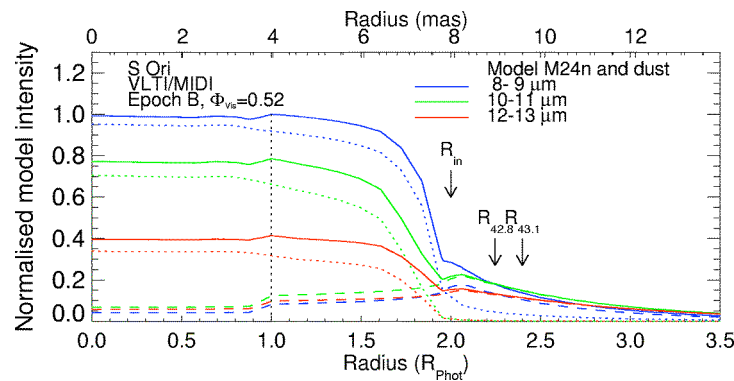
# MIDI observations of S Ori (Dec. 2004 - Dec. 2005)



MIDI total flux



MIDI visibility



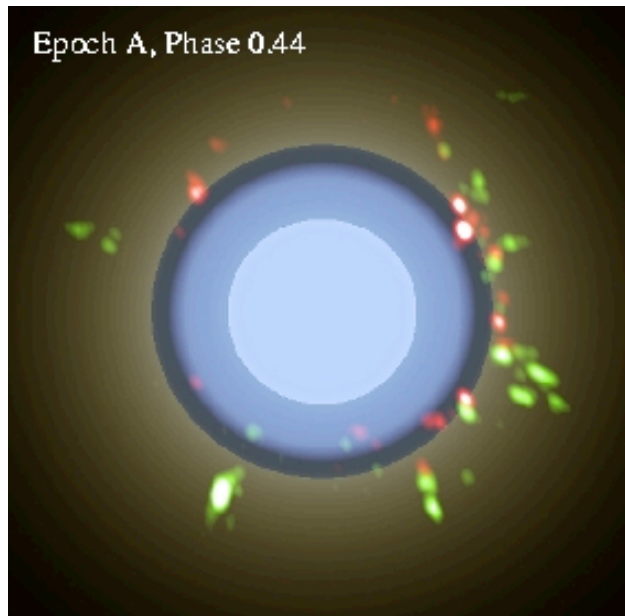
Model intensity

M22  
Al<sub>2</sub>O<sub>3</sub> grains  
 $\tau_V=2.5$   
 $R_{in}=1.8 R_*$   
 $\rho=3.5$

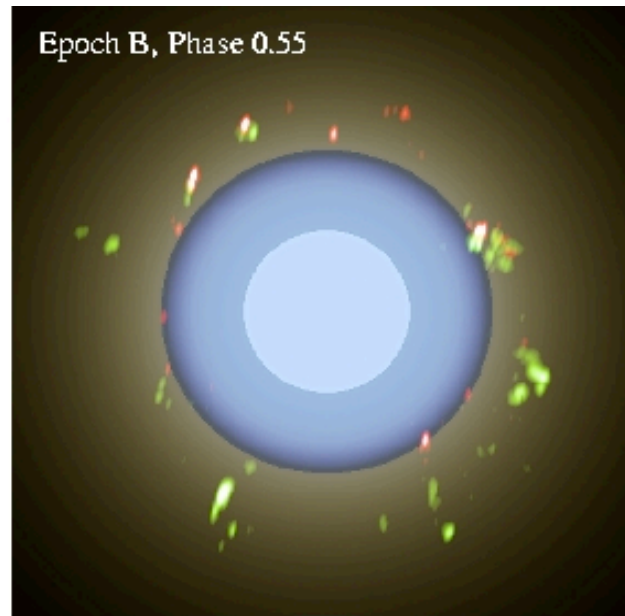
$\Theta_*=9.0$  mas

$R_{43.1}=2.2 R_*$

$R_{42.8}=2.1 R_*$



Epoch B, Phase 0.55



M24n  
Al<sub>2</sub>O<sub>3</sub> grains  
 $\tau_V=2.5$   
 $R_{in}=2.0 R_*$   
 $\rho=3.5$

$\Theta_*=7.9$  mas

$R_{43.1}=2.4 R_*$

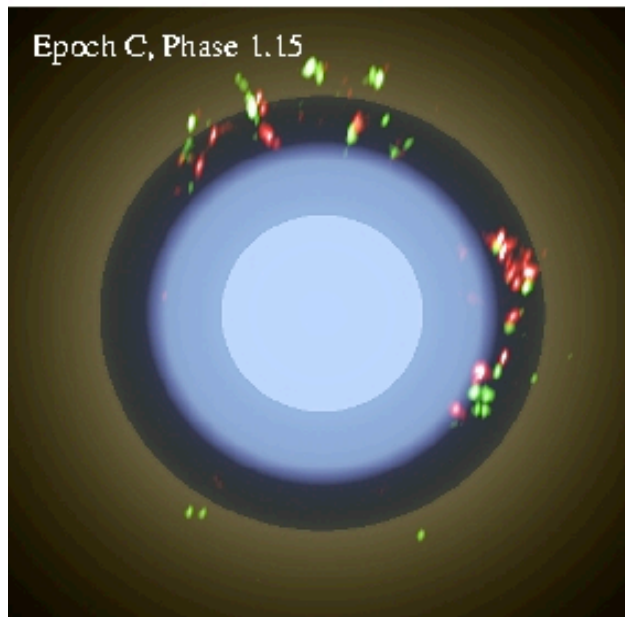
$R_{42.8}=2.3 R_*$

M23n  
Al<sub>2</sub>O<sub>3</sub> grains  
 $\tau_V=1.5$   
 $R_{in}=2.2 R_*$   
 $\rho=3.0$

$\Theta_*=9.7$  mas

$R_{43.1}=2.1 R_*$

$R_{42.8}=1.9 R_*$



Epoch D, Phase 1.27

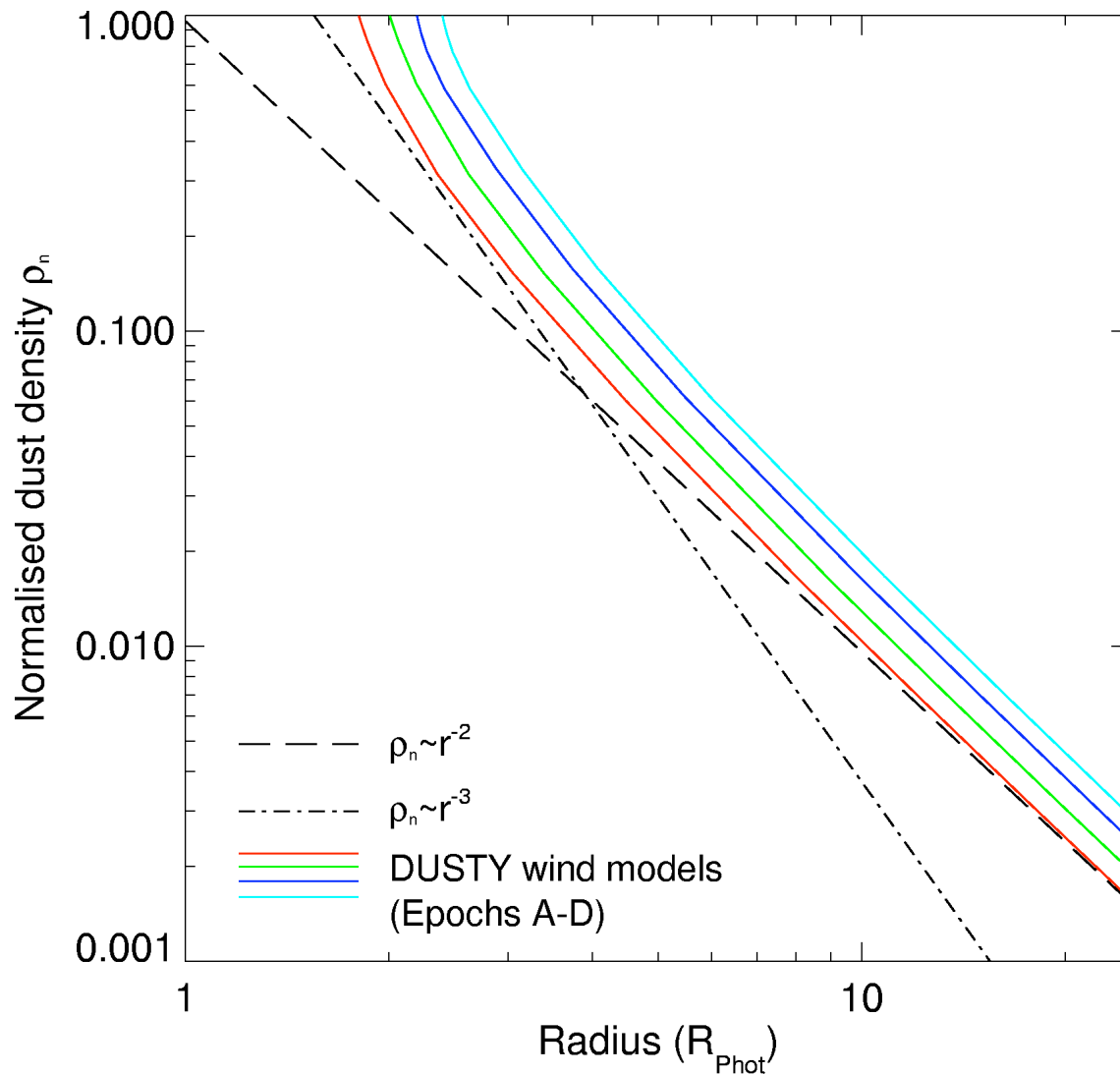


M21n  
Al<sub>2</sub>O<sub>3</sub> grains  
 $\tau_V=1.5$   
 $R_{in}=2.4 R_*$   
 $\rho=2.5$

$\Theta_*=9.5$  mas

(red)  $v=2, J=1-0, 42.8$  GHz and (green)  $v=1, J=1-0, 43.1$  GHz maser images on MIDI model

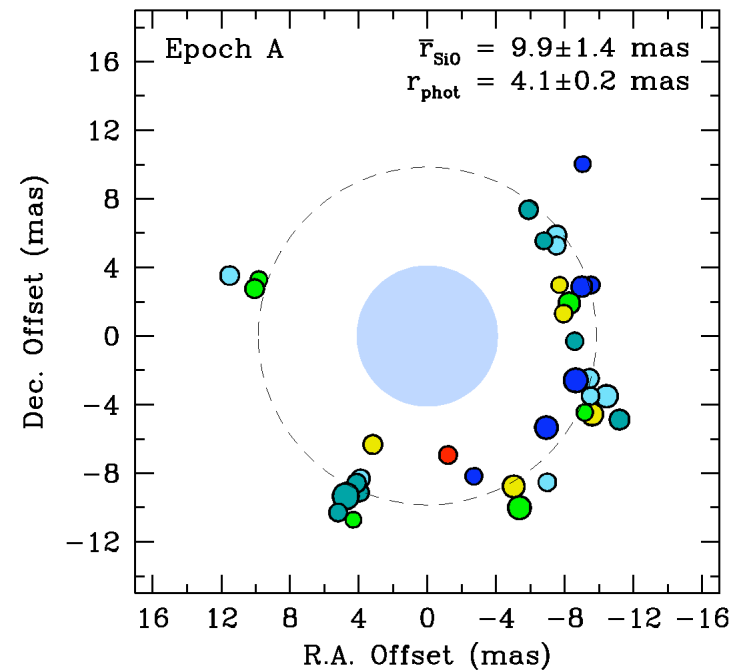
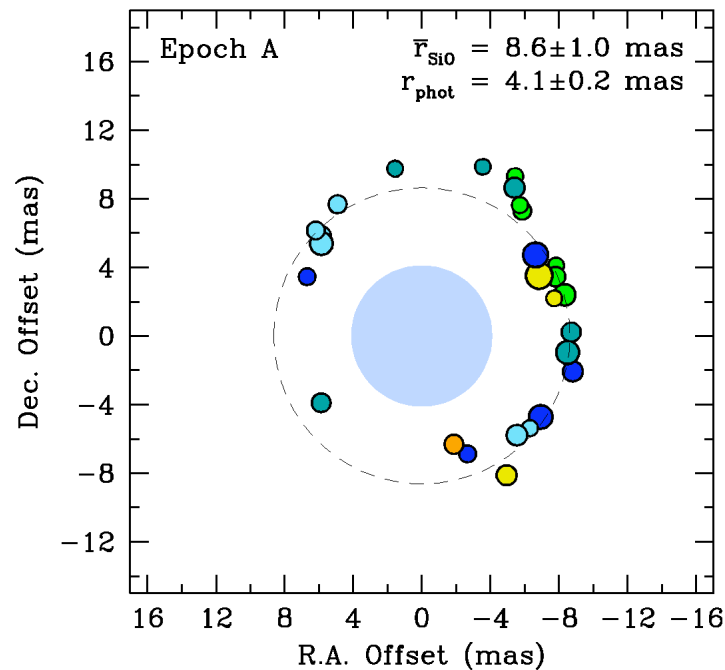
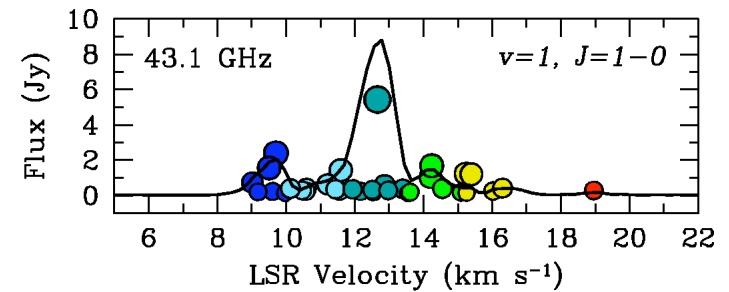
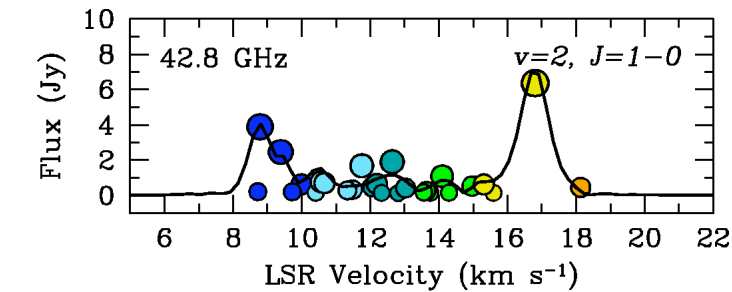
# Density profile derived from a wind model



Wind model calculated with DUSTY (Ivezic & Elitzur 1997), using our best-fit parameters for the dust shell.

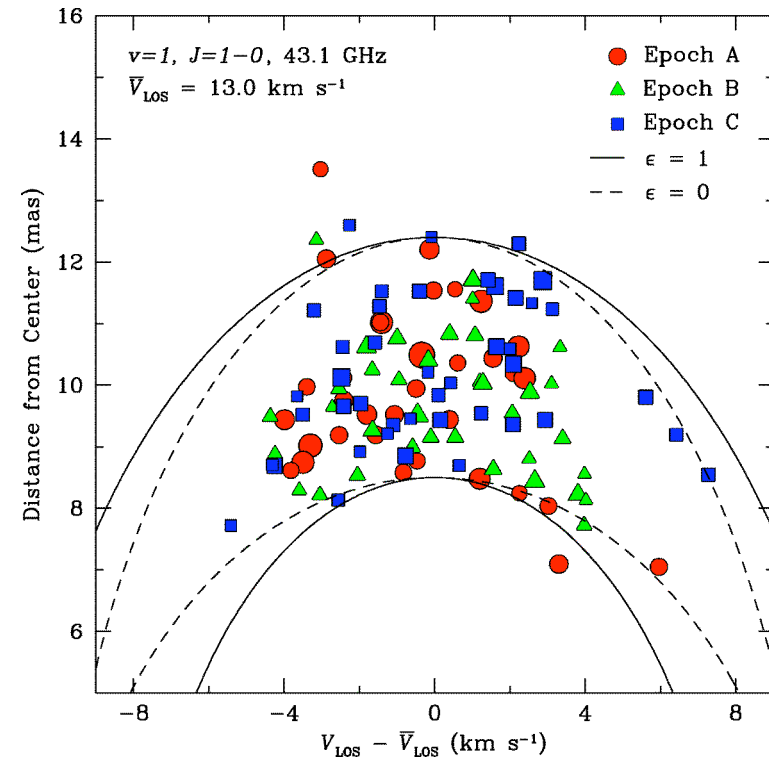
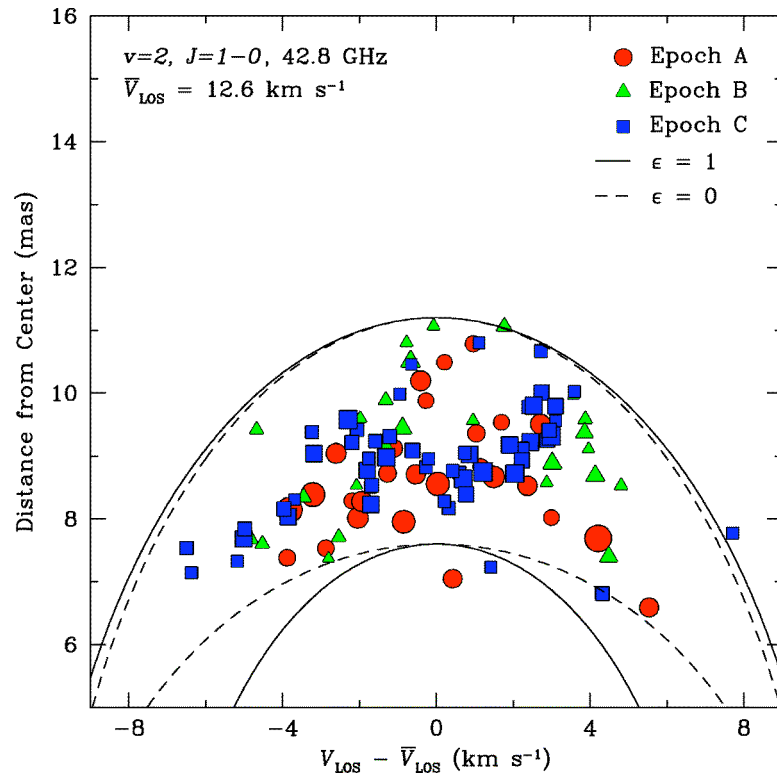
The density profile is proportional to  $r^{-2}$  for distances larger than about 10 stellar radii, but shows steeper gradients closer to the star.

# Velocity structure of the maser spots



The 42.8 GHz masers are systematically at slightly smaller radii than the 43.1 GHz masers. The velocity structure does not show strong systematic features.

# Kinematics of the maser shell



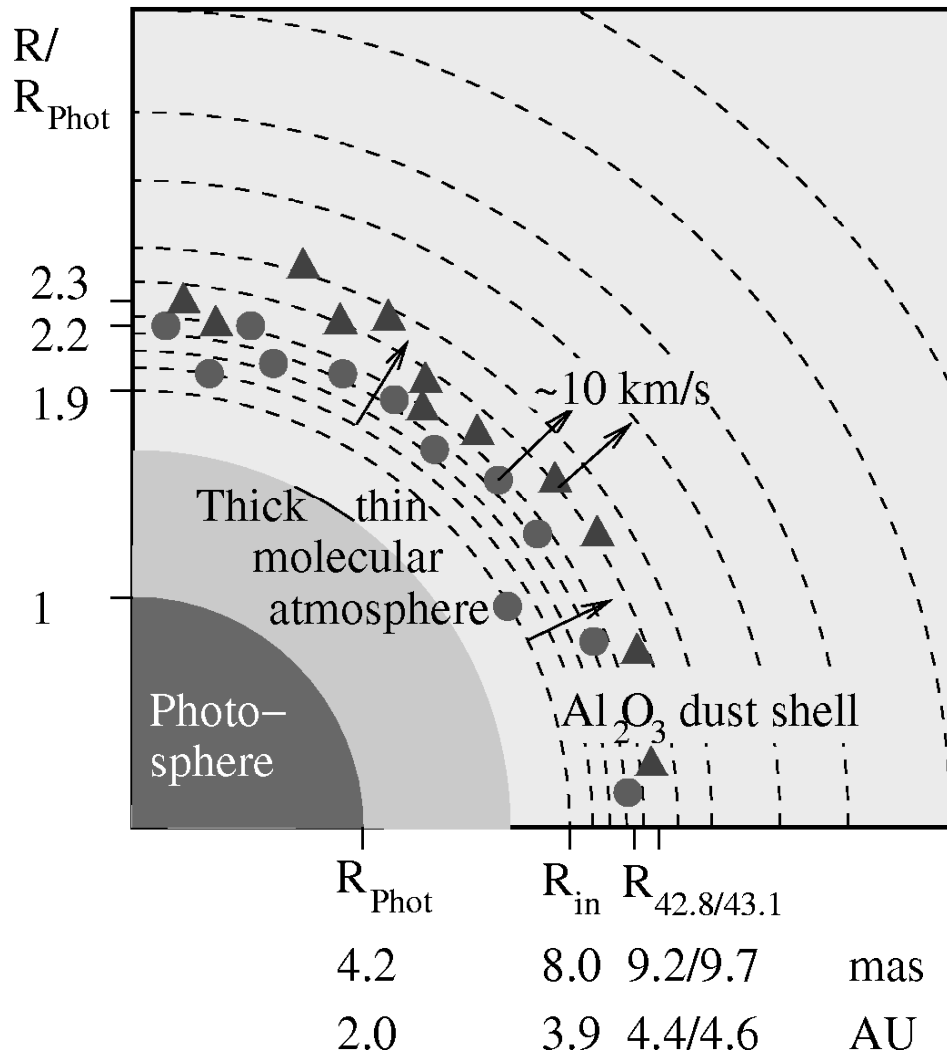
Higher velocity masers are found closer to the star.

Best scenario: Expanding spherical shell with a velocity between 7 km/sec and 10.5 km/sec.

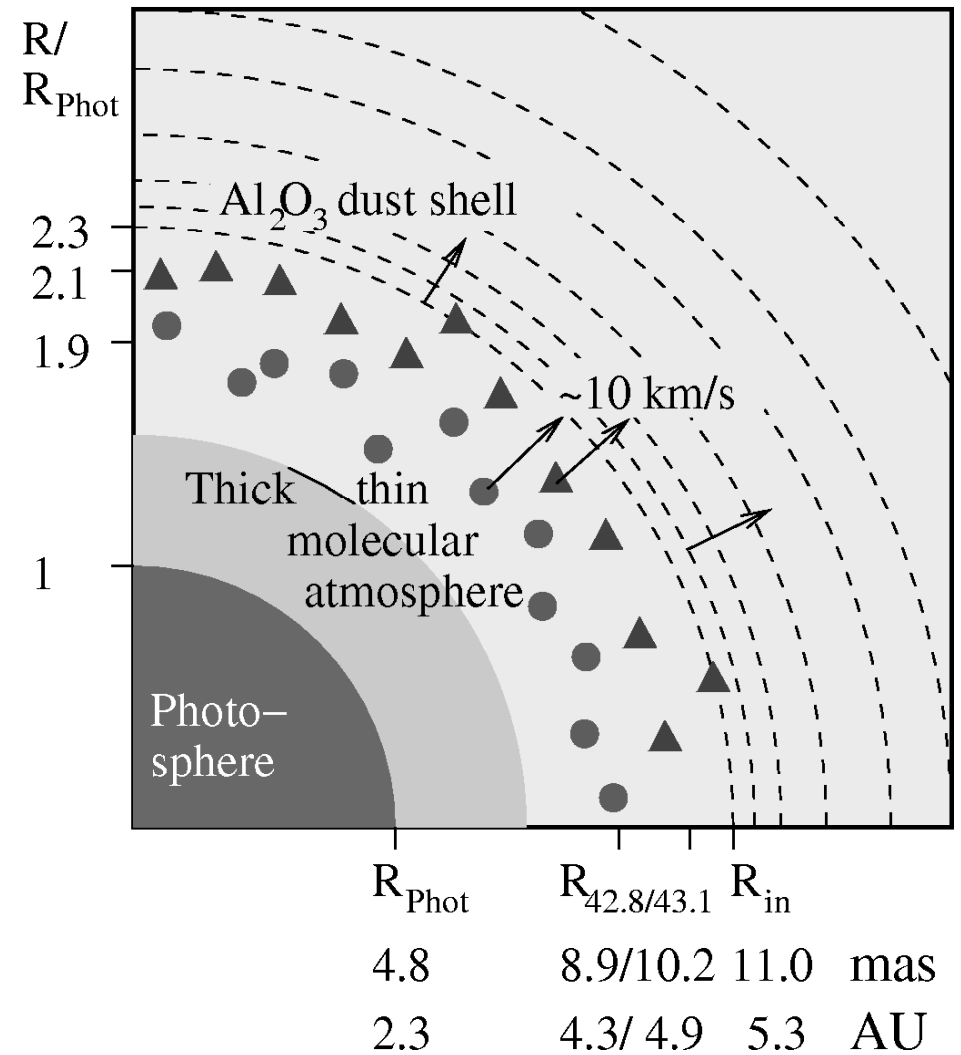
Angle between maser plane and LOS: 90 deg. +/- 25 deg.

# Sketch of the radial structure of S Ori's CSE

S Ori, near visual minimum



S Ori, post visual maximum



## S Ori: Summary of results

- Pilot study (VLT/VINCI NIR + VLBA) showed that the maser shell lies at 2.0 (43.1 GHz) and 1.9 (42.8 GHz) photospheric radii.
- New study shows significant phase dependencies of photospheric radii and dust shell parameters (inner boundary, optical depth, density gradient).
- Both  $\text{Al}_2\text{O}_3$  dust grains and SiO masers form at relatively small radii of  $\sim 1.8$ - $2.4$  photospheric radii. No sign of silicate dust grains.
- The masers and the inner dust shell are co-located near visual minimum.
- The kinematics of the masers suggest some kind of expansion, most likely accelerated.
- Our results suggest increased mass-loss and dust formation near minimum visual phase and a more expanded dust shell after visual maximum.

# The Mira variable GX Mon (Boboltz et al., in preparation)

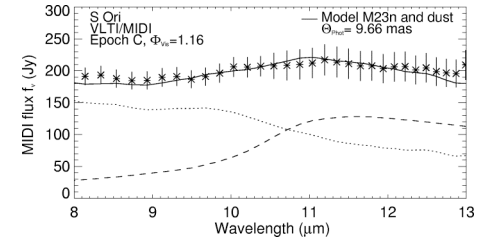
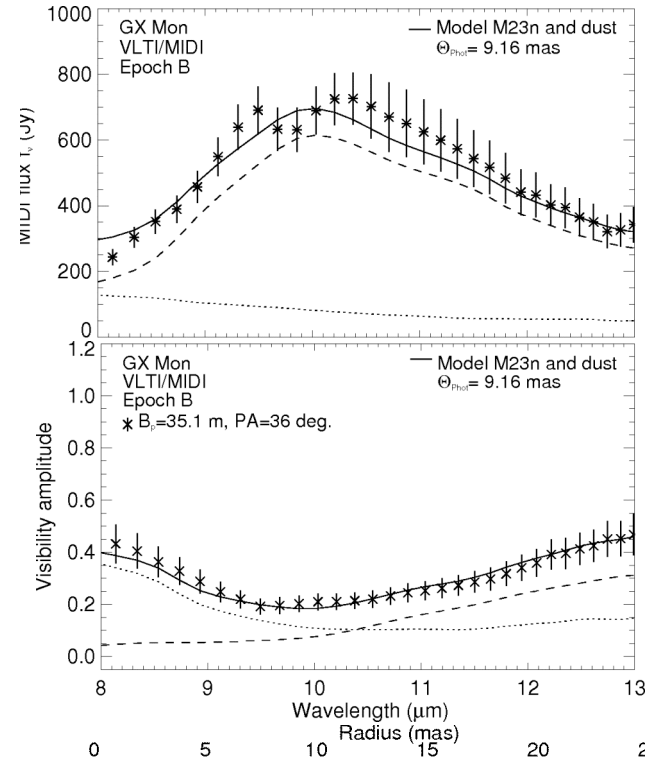
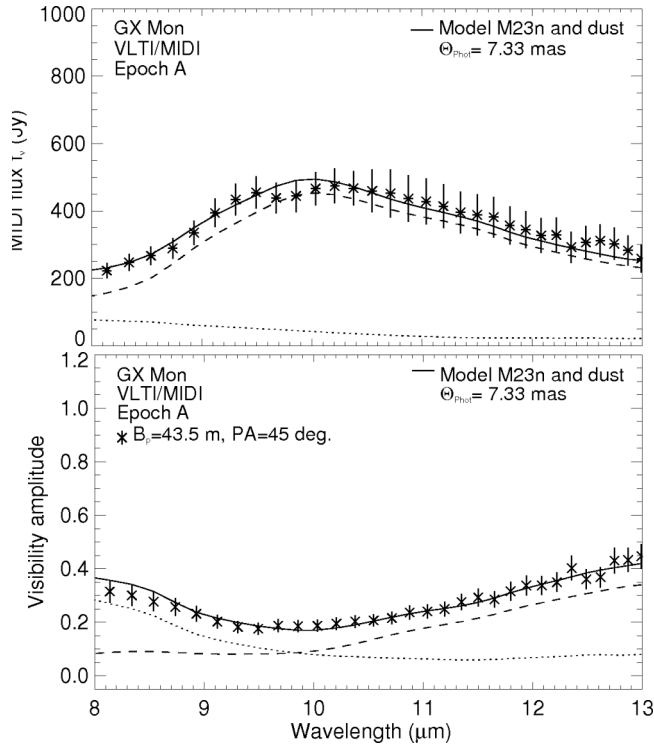
Mira variable with stronger infrared excess compared to S Ori.

2 MIDI/UT epochs: 15 November 2005 & 27 December 2005.  
Observations at additional epochs using MIDI/ATs and  
AMBER/ATs are taken or scheduled.

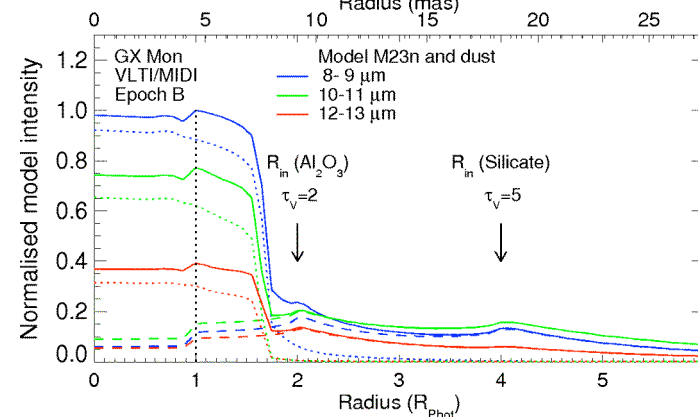
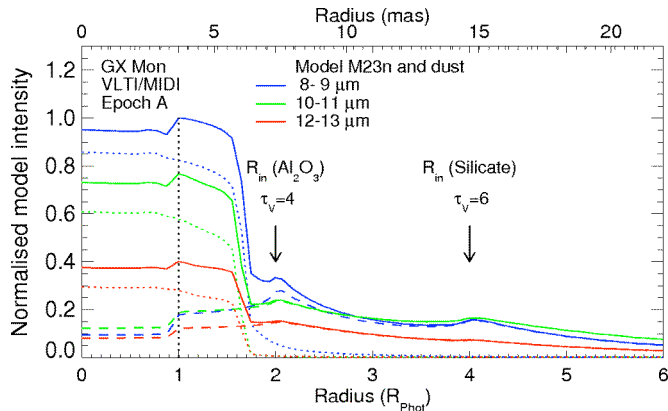
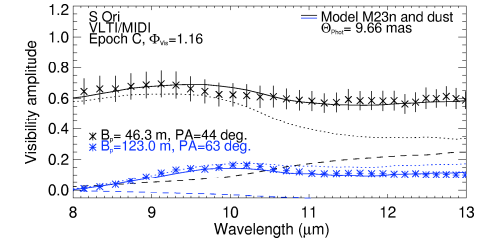
2 VLBA epochs: 8 April 2006 and 18 February 2007, both  
including 42.8 GHz and 43.1 GHz SiO maser (as for S Ori).

Simultaneous H<sub>2</sub>O maser observation on 18 Feb 2007: no signal detected.

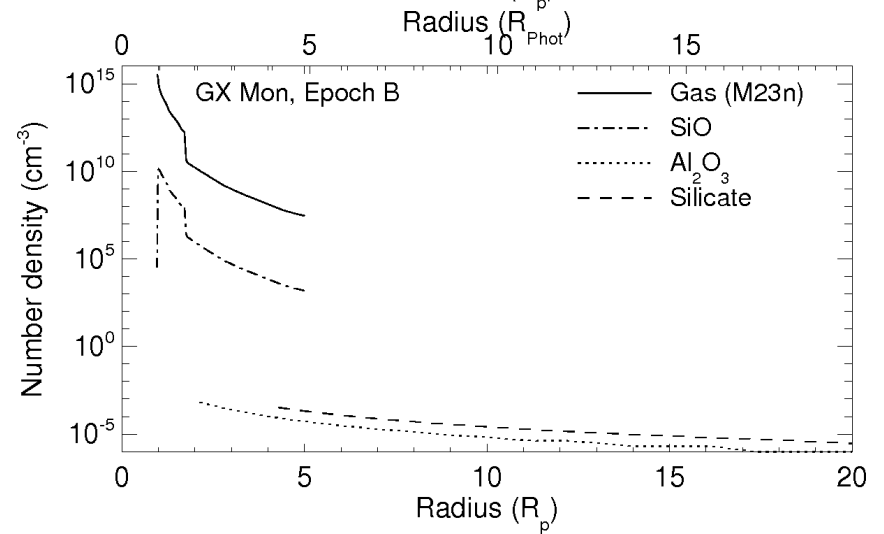
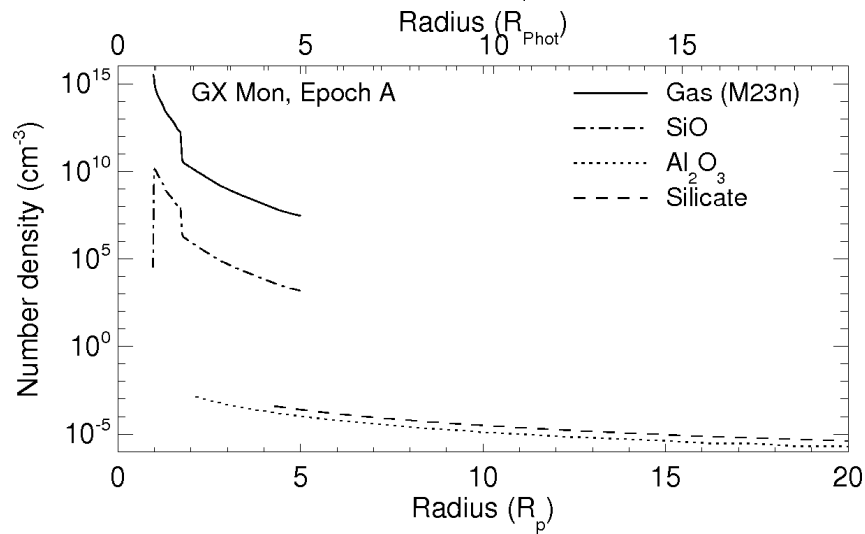
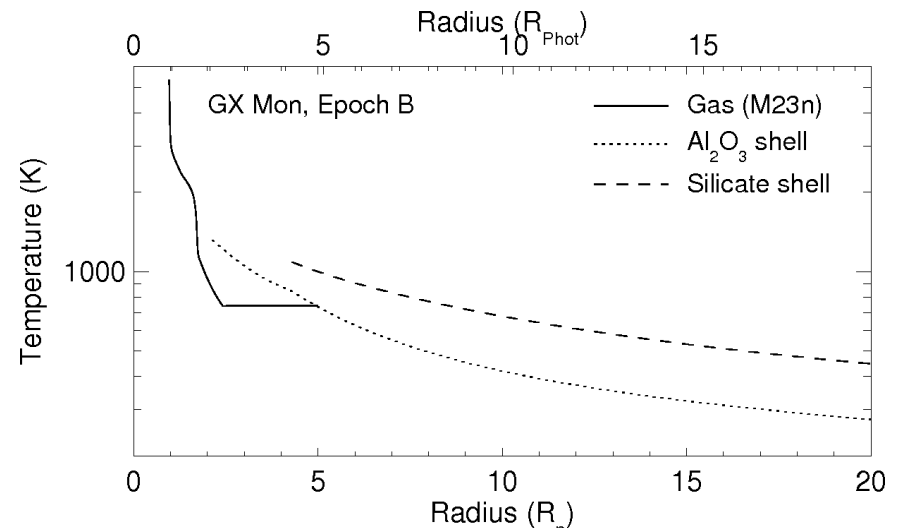
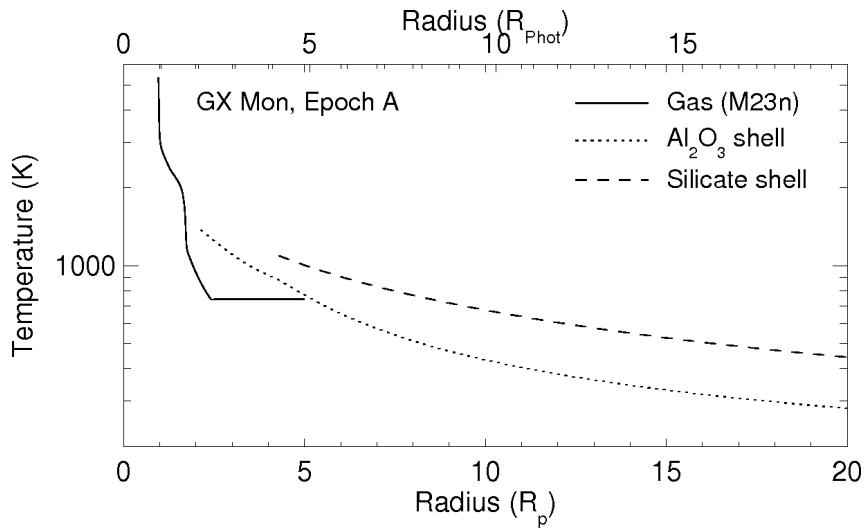
# MIDI observations of GX Mon



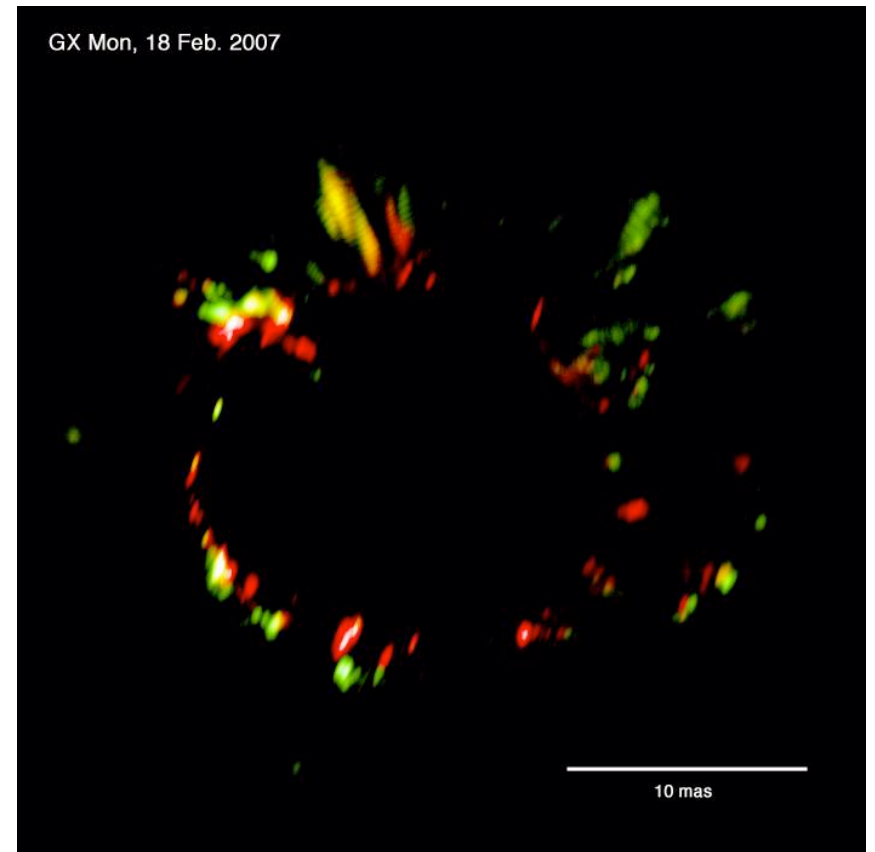
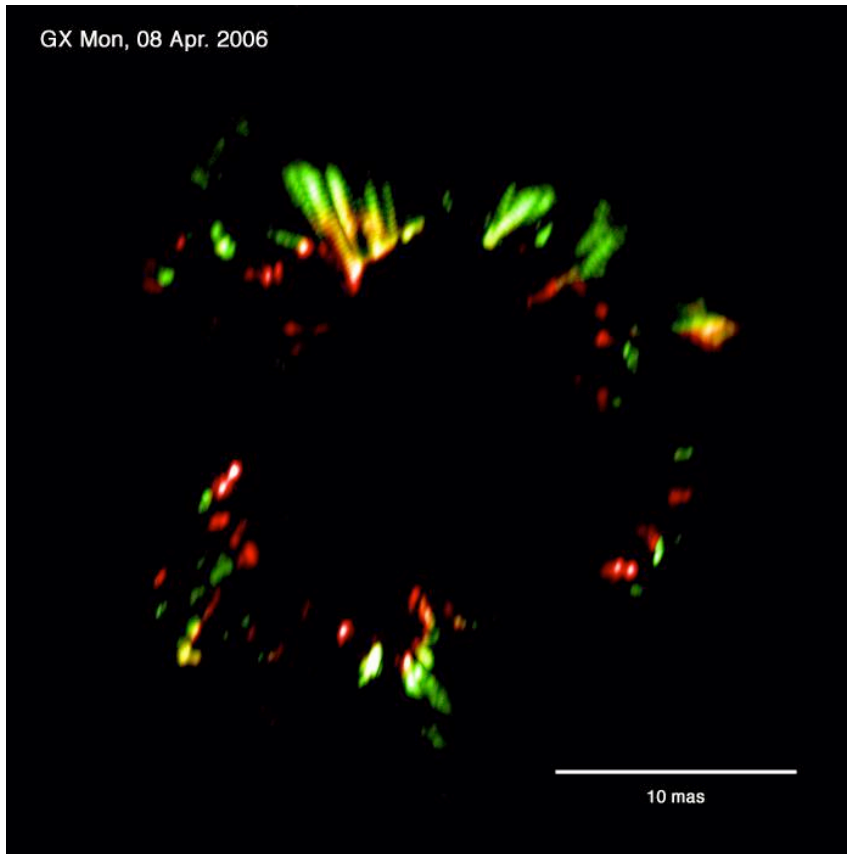
S Ori for comparison



# Model predicted temperature and density

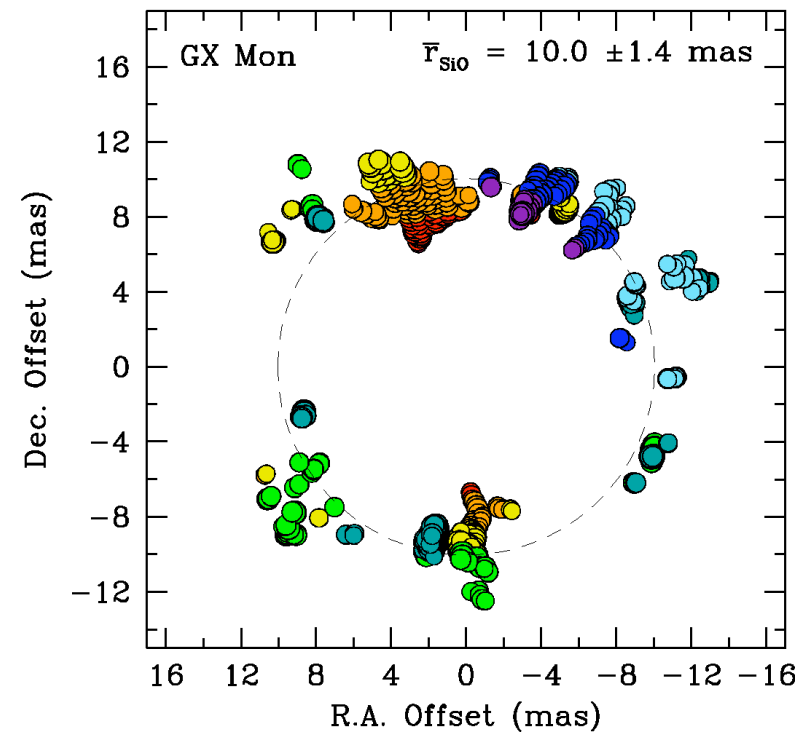
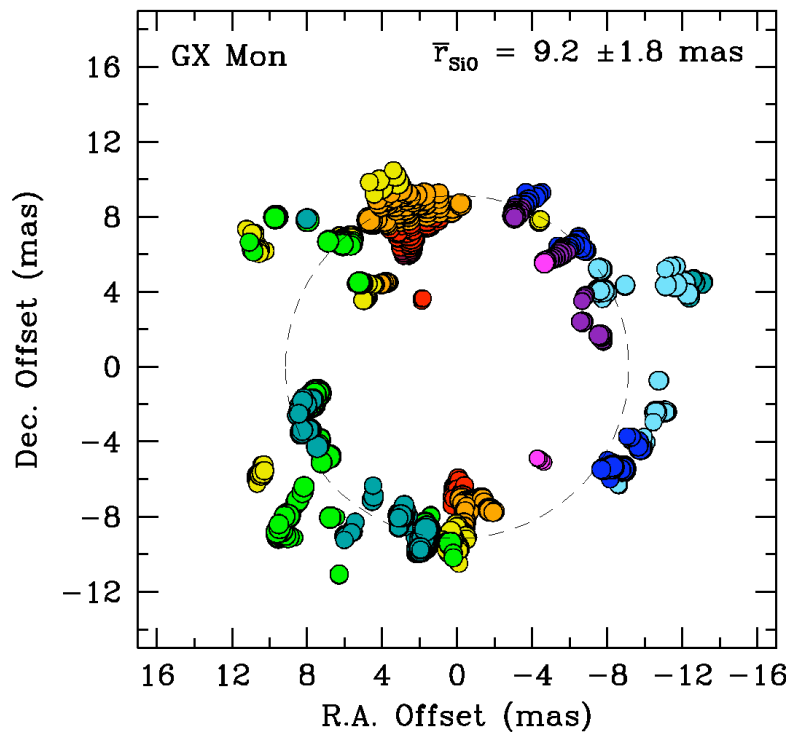
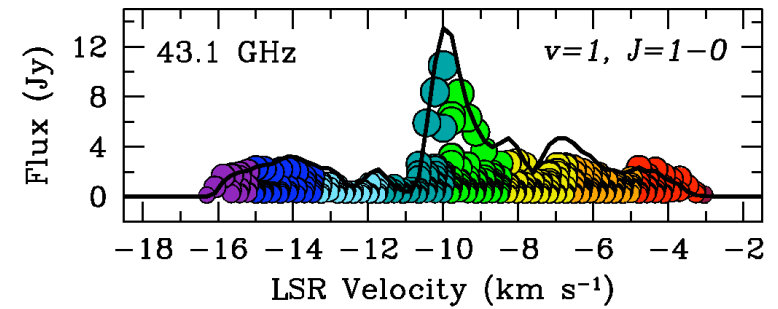
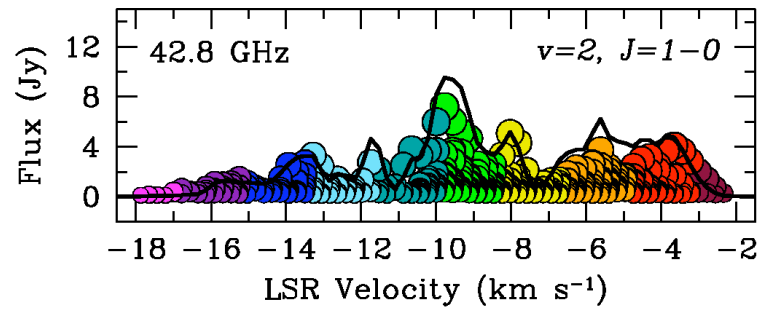


# VLBA observations of GX Mon



(red)  $\nu=2, J=1-0, 42.8$  GHz and (green)  $\nu=1, J=1-0, 43.1$  GHz maser images.

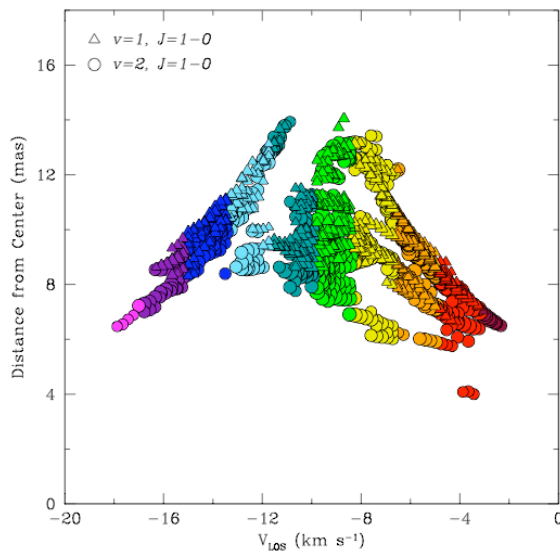
# Velocity structure of the SiO maser toward GX Mon



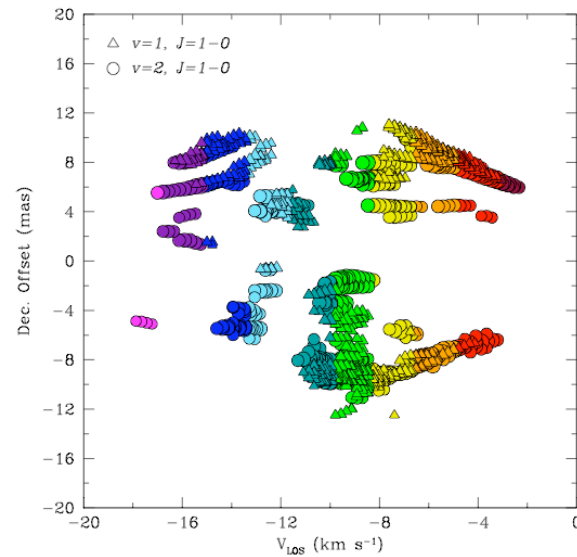
Epoch A, 8 April 2006

# Maser kinematics

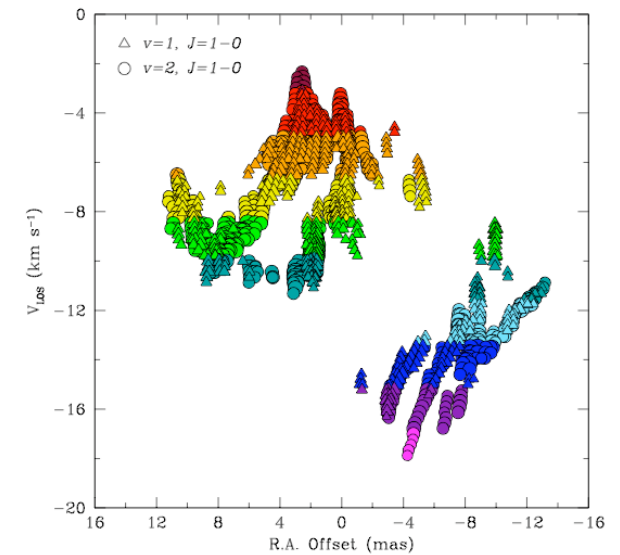
Distance from center  
vs. LOS velocity



Declination offset  
vs. LOS velocity



LOS velocity  
vs. R.A. offset



- Gradient in the velocity as a function of radius (expansion) as for S Ori.
- Preferred axis of symmetry (north-south) with red-shifted masers lying mostly to the east of this axis and blue-shifted masers to the west.

# Summary

- S Ori and GX Mon show significant **phase dependences** of photospheric radii and dust shell parameters.
- S Ori: **SiO masers and  $\text{Al}_2\text{O}_3$  dust grains** form at relatively small radii of  $\sim 1.8\text{-}2.4$  photospheric radii, and **are co-located near visual minimum**.
- Our results of S Ori suggest **increased mass-loss** and dust formation close to the surface **near visual minimum** and an **expanded dust shell after visual maximum**.
- In the case of S Ori, **silicon is not bound in silicates**.
- In the case of GX Mon,  $\text{Al}_2\text{O}_3$  grains at relatively small radii -again co-located with the SiO masers- *and* silicate grains at larger radii can be seen. Clearly higher optical depth than in the case of S Ori. Again phase dependence of dust shell parameters.
- Velocity structure of the maser spots indicate **radial gas expansion** for S Ori and GX Mon. **For GX Mon, there is also a preferred axis of symmetry** of the masers with red-shifted masers lying to the west and blue-shifted to the east..
- To come: Finer monitoring using MIDI/ATs; addition of NIR monitoring using AMBER/ATs; monitoring over more than one period; extension to  $\text{H}_2\text{O}$  and OH maser (wind region); comparison to new modern models of pulsation and dust formation.